LEVEL Ⅱ

Polyphase Pulse Compression Waveforms

F. F. KRETSCHMER, JR. AND B. L. LEWIs

Target Characterstics Branch
Radar Division

DTIC
ELECTE
FEB 1 0 1982
E

January 5, 1982

82 02 10 00

REPORT DOCUMENTATION PAGE		READ INSTRUCTIONS BEFORE COMPLETING FORM
1. REPORT NUMBER NRL Report 8540	2. GOVT ACCESSION NO. AD-A110 751	3. RECIPIENT'S CATALOG NUMBER
4. TITLE (and Subtitle) POLYPHASE PULSE COMPRESSION WAVEFORMS		5. TYPE OF REPORT & PERIOD COVERED Interim report on a continuing NRL problem.
		6. PERFORMING ORG. REPORT NUMBER
7. AUTHOR(s) F. F. Kretschmer, Jr. and B. L. Lewis		8. CONTRACT OR GRANT NUMBER(s)
9. PERFORMING ORGANIZATION NAME AND ADDRESS Naval Research Laboratory Washington, DC 20375		10. PROGRAM ELEMENT, PROJECT, TASK AREA & WORK UNIT NUMBERS 62712N; SF 1214; 491; 55-0605-0
11. CONTROLLING OFFICE NAME AND ADDRESS Naval Sea Systems Command Washington, DC 20362		12. REPORT DATE January 5, 1982
		13. NUMBER OF PAGES 23
14. MONITORING AGENCY NAME & ADDRESS(if different from Controlling Office)		15. SECURITY CLASS. (of this report) UNCLASSIFIED
		15a. DECLASSIFICATION/DOWNGRADING SCHEDULE

16. DISTRIBUTION STATEMENT (of this Report)

Approved for public release; distribution unlimited.

17. DISTRIBUTION STATEMENT (of the abstract entered in Block 20, if different from Report)

18. SUPPLEMENTARY NOTES

19. KEY WORDS (Continue on reverse side if necessary and identify by block number)

Waveform design
Radar
Signal processing

20. ABSTRACT (Continue on reverse side if necessary and identify by block number)

This report discusses radar pulse-compression waveforms and the advantages of digital polyphase codes over analog waveforms. The Frank polyphase code is investigated in detail and generalized. It is shown that the relative sidelobes of a compressed Frank-coded waveform degrade in the presence of bandlimiting prior to pulse compression. The P1 and P2 polyphase codes are shown to be tolerant of precompression bandlimitation. Finally, applications for these polyphase codes are discussed.

DD FORM 1473 EDITION OF 1 NOV 65 IS OBSOLETE
1 JAN 73
S/N 0102-014-6601

CONTENTS

iii

POLYPHASE PULSE COMPRESSION WAVEFORMS

INTRODUCTION

Pulse-compression techniques have been recognized for some time as a means of obtaining sufficient average power on targets for detection, while retaining a desired range resolution with peak-power limited radars. In radar practice, waveforms having a constant amplitude are usually generated to obtain maximum transmitted signal power. Under these conditions, a constant-amplitude pulse of length T can be compressed to a pulse of length τ by phase modulating the signal so that the spectral bandwidth is approximately equal to $1/\tau$. The resultant pulse compression ratio ρ is then equal to T/τ or TB, where B is the bandwidth which is equal to $1/\tau$. This phase modulation is commonly achieved by a linear fm, or chirp waveform where the phase varies quadratically with time so that the instantaneous frequency varies linearly with time. The frequency spectrum of the chirp signal is nearly rectangular with a width B, and the compressed pulse is approximately equal to the Fourier transform of the frequency spectrum.

The resultant sin t/t pulse has large time sidelobes which are capable of masking a nearby weak target and therefore a weighting, such as the Taylor weighting, is generally applied to reduce the sidelobe levels [1,2]. These weights symmetrically reduce the amplitude of the rectangular spectrum at the edges of the band and result in lower sidelobes. A weighting applied to the received waveform results in a mismatch which causes a loss typically on the order of 1 to 2 dB in the output peak-signal to noise ratio. Also the pulsewidth of the compressed pulse is widened.

Another common pulse-compression waveform is the binary-phase-coded waveform where the carrier is modulated by $0°$ and $180°$ phases. Pseudo-random binary sequences may be generated by using shift registers and, in general, the best binary pseudo-random sequences have a peak sidelobe level which is down from the main response by a factor of ρ. These codes are useful where a thumbtack ambiguity surface is desired. The doppler response of these codes is generally poor, and multiple doppler channels are required over the range of expected doppler returns.

Complementary codes generally consist of two binary sequences which are combined after pulse compression and result in low sidelobes. However, these codes likewise have a poor doppler response and are not generally useful in radar because of the need to separate the two codes in frequency, time, or polarization to permit them to be compressed separately. This separation can cause decorrelation by radar targets or distributed clutter and prevent cancellation of the sidelobes of the combined compressed pulses.

POLYPHASE CODES AND DIGITAL PULSE COMPRESSION

Advantages

The polyphase-coded waveforms discussed in this report offer many advantages over analog pulse-compression waveforms. These advantages include the ability to achieve low sidelobes without weighting, although weighting can be applied easily to achieve still lower sidelobes. Also, the polyphase coded waveforms are. (a) relatively doppler tolerant; (b) easily implemented; (c) have no

reflections, as there may be in acoustic delay lines; (d) relatively insensitive to phase errors; and (e) enjoy the advantages of digital processing. These advantages include reliability, reproducibility and compatibility with other digital signal-processing functions, such as moving-target indicator (MTI) and pulse doppler. The use of digital pulse compression allows the digital MTI to precede the digital pulse compressor without requiring multiple A/D and D/A conversions. Also, placing the MTI before the pulse compressor reduces the dynamic range requirements of the MTI.

Equivalance to Analog Processing

In this section we denote by a_i the complex (I,Q) baseband samples of a received uncompressed pulse having an intermediate frequency (IF) bandwidth B. The complex video bandwidth is $B/2$ and it is assumed that samples are taken every $1/B$ s. Recalling that the optimization criterion leading to the matched filter maximizes the output peak signal to average noise power ratio S_p/N, which is given by $2E/N_0$, [2] it will be shown that digital processing achieves the same value for S_p/N.

For the digital case, the peak signal output power at the matchpoint is given by

$$S_p = k \left(\sum a_i a_i^* \right)^2 = k \left(\sum |a_i|^2 \right)^2 \tag{1}$$

where k is a constant. In the above and following summations, the index ranges from 1 to p. The output noise voltage of the matched filter is

$$n = k \sum a_i^* n_i \tag{2}$$

where n_i is equal to the complex value of the ith noise sample. The average noise power in the signal envelope is then

$$|n|^2 = k \sum_i \sum_j a_i^* a_j n_i n_j^* . \tag{3}$$

For complex, zero-mean, band-limited white noise, the coefficients are uncorrelated for a sampling interval T_s equal to $1/B$ and Eq. (3) becomes

$$\overline{|n|^2} = k \overline{|n_i|^2} \sum |a_i|^2 . \tag{4}$$

The noise powers of interest may be computed by considering the narrowband representation for the IF noise waveform $x(t)$ given by

$$x(t) = n_I(t) \cos \omega_0 t + n_Q(t) \sin \omega_0 t$$

2

where n_I and n_Q are slowly varying independent Gaussian noise processes; n_I and n_Q have 0 means and equal variances σ_I^2 and σ_Q^2, which are also denoted by σ^2. The average noise power is

$$\sigma_x^2 = \left(\sigma_I^2 + \sigma_Q^2\right) \Big/ 2 = \sigma^2$$

$$= KT_0 FB = N_0 B , \tag{5}$$

where K is the Boltzman constant, T_0 is the standard noise temperature, and F is the noise figure. Also,

$$\overline{|n_i|^2} = \sigma_I^2 + \sigma_Q^2 = 2\sigma^2 = 2N_0 B . \tag{6}$$

Substituting Eq. (6) in Eq. (4), the average envelope noise power is

$$\overline{|n|^2} = k 2N_0 B \sum |a_i|^2 , \tag{7}$$

and using the relation that N is equal to one half of the envelope noise power computed in Eq. (7), we have

$$\frac{S_p}{N} = \frac{\sum |a_i|^2}{N_0 B} . \tag{8}$$

From Reference 3,

$$\sum |a_i|^2 = 2BE$$

so that

$$\frac{S_p}{N} = \frac{2E}{N_0} \tag{9}$$

is in agreement with the an   .

Note that although the ratio S_p/N is the same for the analog and digital compressed pulses, the sidelobes are generally different.

THE FRANK-POLYPHASE-CODED WAVEFORM AND A COMPARISON WITH OTHER WAVEFORMS [4,5]

It will be shown that the phases of the Frank-coded waveforms are the same as the appropriately sampled phases of a step-chirp waveform. These phases are shown to be the same as the steering phases of a discrete Fourier transform (DFT), which means that this code can be generated efficiently or compressed by using a fast Fourier transform (FFT).

The doppler properties of the Frank code are similar to those of a step-chirp waveform and the Frank-coded waveform is more tolerant of doppler than the pseudo-random binary codes or the nonlinear chirp waveforms [1]. The doppler response of the compressed Frank-coded waveform is down approximately 4 dB, like the binary code, when the total accumulated phase shift due to doppler across the uncompressed pulse is π. The binary-code response continues to decrease with increasing doppler shift, while the Frank-code response increases to nearly full amplitude for a phase shift of 2π. The Frank-code response is cyclic with troughs occurring at odd multiples of π and with peaks occurring at multiples of 2π phase shift across the uncompressed pulse. This was not recognized in the publisher literature [1,6] since the doppler cuts were taken at much larger doppler intervals. The cyclic nature of the Frank code doppler response can be easily compensated to further improve the doppler response.

It is later shown that for a Frank code consisting of $N^2 = \rho$ phases, the peak sidelobe is down from the main response by a factor of $(\rho\pi^2)$. The best pseudo-random shift-register binary codes have peak sidelobes that are down by a factor which approaches ρ so that the Frank-code waveforms nave lower peak and rms sidelobes than the binary codes. This means that, in a distributed clutter environment, the clutter received via the Frank-code-waveform sidelobes is less than that received via the binary-waveform sidelobes.

The sidelobe level of the Frank code decreases with increasing pulse-compression ratio and low sidelobes are achieved without weighting. However, a further reduction in the sidelobe level can be achieved easily by weighting. In contrast, the chirp signal is generally weighted and there is an attendant loss in S/N and widening of the pulsewidth. This section of this report concludes with a discussion of polyphase-code sidelobe reduction techniques and the sensitivity of polyphase codes to phase errors.

Frank-Polyphase-Coded Waveform

The Frank-polyphase-coded waveform may be described and generalized by considering a hypothetically sampled step-chirp waveform [4]. The Frank code was not originally described in this manner, but was given in terms of the elements of a matrix [7]. As an example, consider a four-frequency step-chirp waveform as shown in Fig. 1(b) where the F_i's denote frequency tones. In this waveform, the frequency steps are equal to the reciprocal of the tone duration $4\tau_c$, where τ_c denotes the compressed pulse width. Assuming this waveform has been beat to baseband I and Q using a synchronous oscillator having a frequency the same as the first tone frequency, the resultant phase-vs-time characteristic consists of four linear sections as shown on Fig. 1(a). The corresponding baseband frequencies are the subharmonics of the frequency $1/\tau_c$. If the baseband phases of the step-chirp waveforms are sampled every τ_c s and held for τ_c s, the phase sequence shown in Fig. 1(c) is obtained. This sequence of phases constitutes the phases of a Frank code for $N = 4$, corresponding to the four baseband frequencies of the hypothetical step-chirp waveform. The actual transmitted Frank-coded-waveform consists of a carrier whose phase is modulated according to the indicated baseband waveform sequence. For each frequency, or section, of the step-chirp phase characteristic, a phase group consisting of N phase samples is obtained and the total number of code phases is N^2 which is equal to the pulse-compression ratio. Note that the phase increments within the four phase groups are $0°$, $90°$, $180°$ and $270°$. However, the phases of the last group are ambiguous ($>180°$) and appear as $-90°$ phase steps or as the conjugate of the F_1 group of phases, which corresponds to the lower sideband of F_1. The last group of phases appears, because of the ambiguity, to complete one $360°$ counterclockwise rotation rather than the $(N-1)$ rotations of the end frequency of the step-chirp waveform.
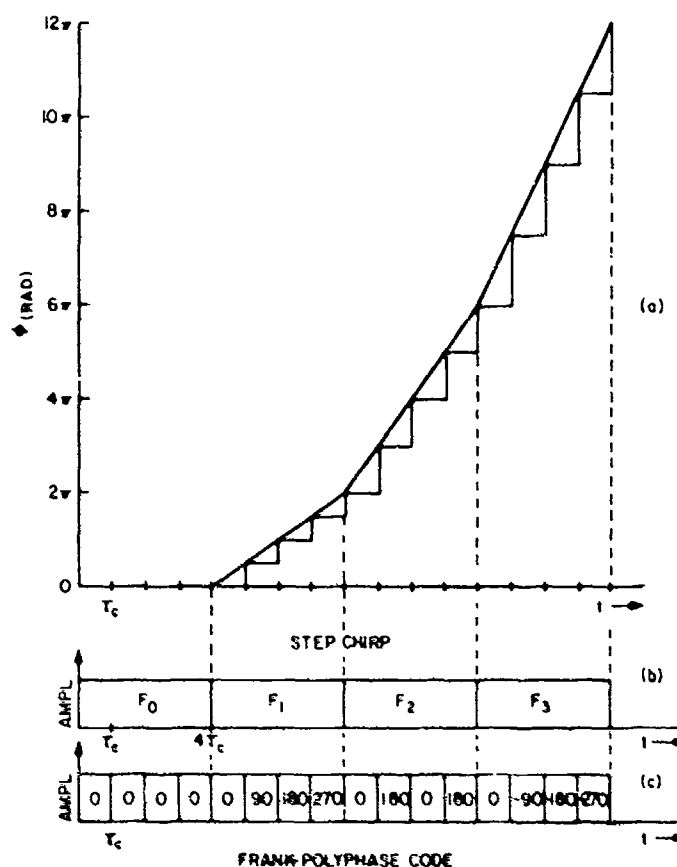
Fig. 1 — Step-chirp and Frank-polyphase-code relationships

The Frank-code phases may be stated mathematically as follows. The phase of the ith code element in the jth phase group, or t aseband frequency, is

$$(2\pi/N)(i - 1)(j - 1) \tag{10}$$

where the index i ranges from 1 to N for each of the values of j ranging from 1 to N. An example of a Frank-code pulse generation for N = 3 is shown in Fig. 2. The Frank-code phases are the same as the negative of the steering phases of an N point DFT where the jth frequency coefficient is:

$$F_j = \sum_{i=1}^{N} a_i e^{-j\frac{2\pi}{N}(i-1)(j-1)} \tag{11}$$

where a_i is the ith complex input time sample. This means that a considerable savings in hardware can be achieved by using the efficiency of an FFT.

The matched filter output for an N = 10 or 100-element Frank code is shown in Fig. 3. This figure and the following figures showing the compressed pulse were obtained by sampling the input baseband waveform once per code element or per reciprocal bandwidth unless stated otherwise. Using a discrete-time matched filter the output signal is also a discrete-time sampled signal.
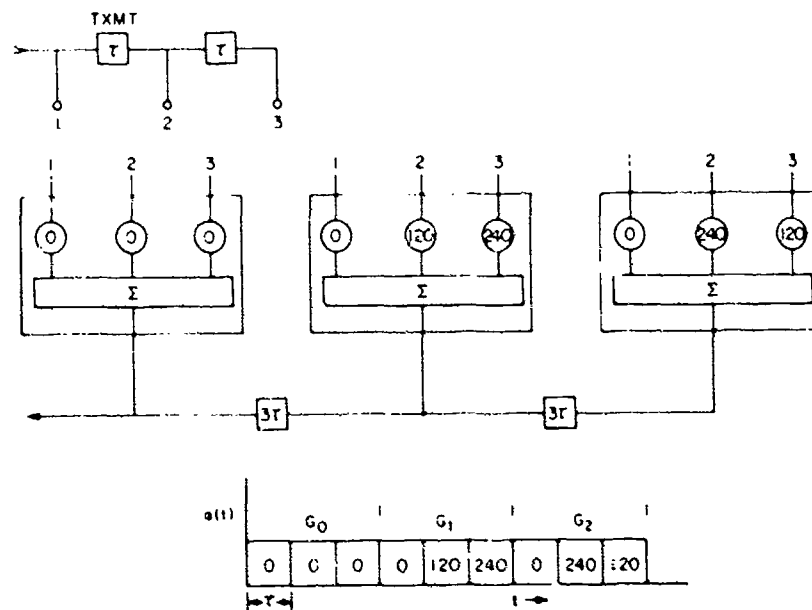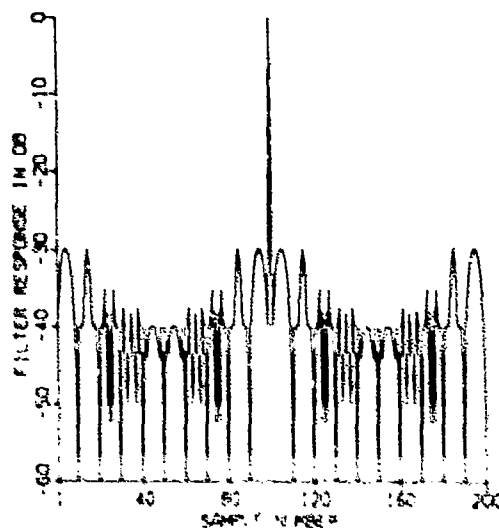
5

Fig. 2 — Simplified Frank-code generation

Fig. 3 — Compressed pulse of 100-element Frank-polyphase code

However, for ease of plotting and viewing, the points were connected by straight lines. The four sidelobe peaks on each half of the match point (peak response) are of equal magnitude. The first peak sidelobe at sample number 5 in Fig. 3 occurs as the last phase group having $-36°$ phase increments indexes halfway into the first phase group of zero phase vectors in the autocorrelation process. In general, at sample number $N/2$, there are $N/2$ vectors adding to complete a half circle. The end phase group indexing into the first phase group of $0°$ vectors makes an approximate circle since the phases of the last phase group make only one rotation as stated previously. The peak sidelobe amplitude may be approximated by the diameter D of the circle from the relation,

$$\text{Perimeter} = N = \pi D \tag{13}$$

$$\text{or} \quad D = N/\pi . \tag{14}$$

At the match point the amplitude is N^2 so that the peak-sidelobe to peak-response power ratio R is

$$R = \frac{N^4}{(N/\pi)^2} = N^2 \pi^2 = \rho \pi^2 . \tag{15}$$

For a 100-element Frank code, this ratio is approximately 30 dB as shown in Fig. 3.

Had the phases of the polyphase-coded waveform been generated by using the phases of step-chirp phase characteristics sampled at 1/5 of the interval used for the Frank code, the compressed code would appear as shown in Fig. 4. In this figure, five samples are equal in time to one sample in Fig. 3. Note in Fig. 4 that the near-in sidelobes are approximately 13 dB and that the envelope of the sidelobe peaks is approximately that of a sin x/x pulse. The 13-dB sidelobes also appear for an oversampling of 2:1. Also note that the compressed pulsewidth in Fig. 4 has not decreased since it is determined by the underlying bandwidth of the step-chirp waveform.

A comparison between the Frank code and a "good" binary code may be made by referring to Figs. 5 and 6 which have similar pulse-compression ratios. Fig. 7 shows a comparison of the
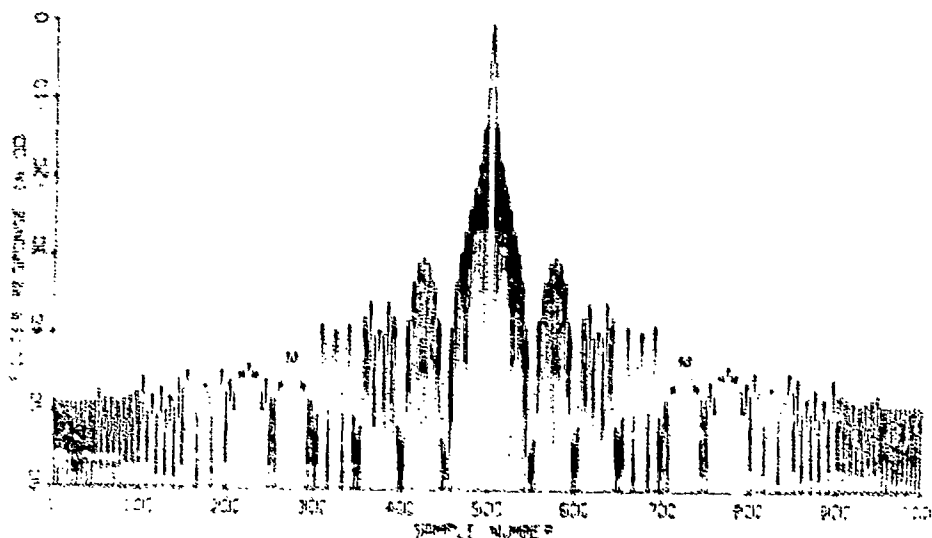

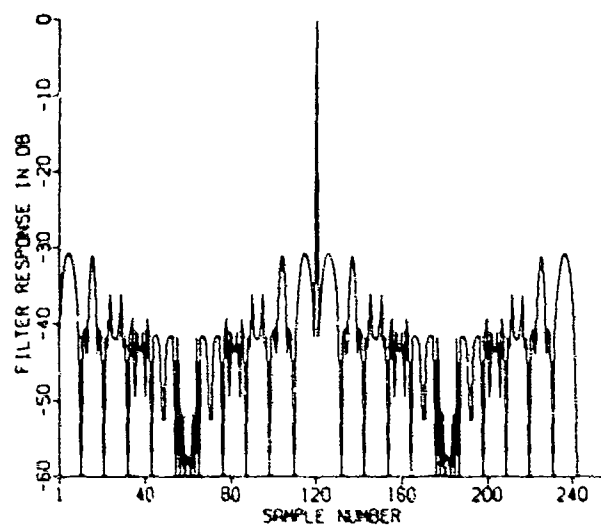Fig 4 — Compressed pulse of oversampled step-chirp (5:1)

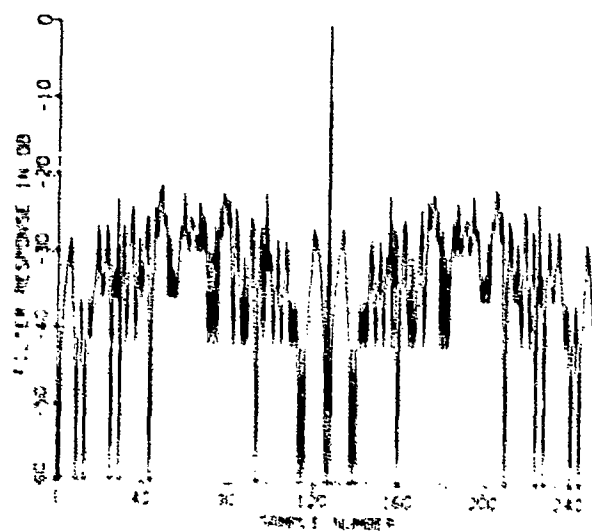Fig. 5 — Compressed pulse of 121-element Frank code

Fig. 6 — Compressed pulse of 127-element binary
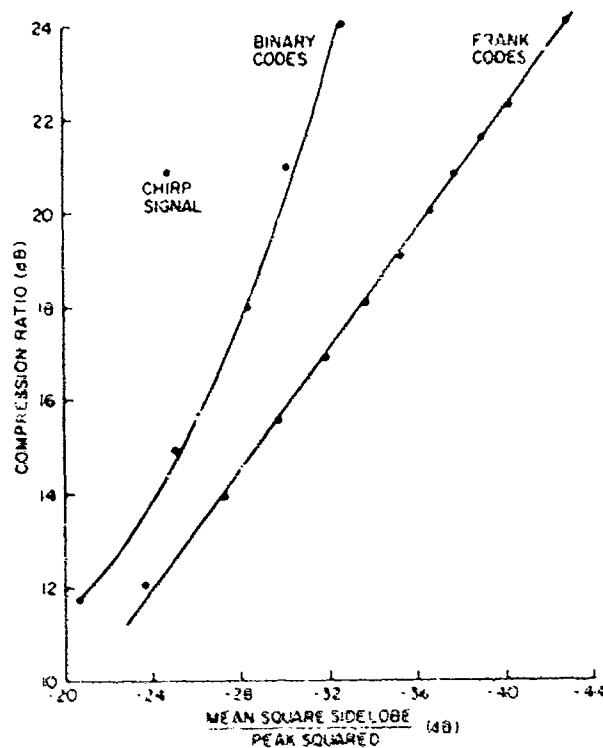shift register code

Fig. 7 - Comparison of mean-squared sidelobes

mean-square sidelobe power of the two codes. From this, one can see that better performance is achieved with the Frank code in a distributed clutter environment where clutter is introduced via the sidelobes of the compressed pulse. Also shown in Fig. 7 is a point, for the sake of comparison, for an unweighted chirp signal. The relatively high mean-square sidelobe level is due to the high near-in sidelobes.

Sidelobe Reduction Techniques

Various methods have been investigated to cause a further reduction of the Frank-code sidelobe levels. One method is based on a least-squares technique [8] whereby, for a given input waveform, the filter coefficients are found such that the output of the compression filter best approximates an idealized impulse function. This technique can also be applied to binary waveforms. It was found that this technique did not produce a symmetrical output waveform for a Frank-polyphase-coded input waveform. However, for the new P1 coded waveform, to be discussed in this report, a small sidelobe reduction was achieved.

Another method for reducing the sidelobes was investigated by Somaini and Ackroyd [9]. Their approach was to perturb the phases of a Frank code by search methods until an improved autocorrelation function was achieved. Using their resultant perturbed waveform, the peak sidelobes for a 100 element code were reduced from 30 to approximately 36 dB.

The shortcomings of the preceding techniques are that the doppler responses are not quite as good as the Frank code and that the filter cannot be implemented using FFT efficiency. The most effective method that has been found for reducing the sidelobes is achieved by simply weighting the output frequency ports of the FFT compression filter. Any of the recognized weightings can be used in this manner. Fig. 8 shows the results of using a cosine-on-a pedestal (of 0.4) weighting on a 100-element Frank-coded waveform. The peak signal is reduced as shown but the loss in signal-to-noise ratio (S/N) is small.

Doppler Response of Frank Code

A partial ambiguity function for a 100-element Frank code is shown in Fig. 9 which shows the amplitude in dB of a matched-filter output for given doppler shifts of the input. The doppler is normalized to the signal bandwidth and the delay axis is normalized to the uncompressed pulse length. The vertical scale ranges from 0 dB to -60 dB, and the -30-dB sidelobes for 0 doppler are evident. A front view is shown in Fig. 10 where the sidelobes are plotted down to the -30-dB level. The normalized doppler shift of -0.05 shown in this figure corresponds to a mach-50 target for an L-band radar having a signal bandwidth of 2 MHz. The first doppler cut shown in the literature [6] is taken at this normalized doppler and the resultant high-peak sidelobes have perhaps discouraged usage of the Frank code. The region shown between 0 and mach-5 doppler and a delay interval of ±0.3 is of interest, and it is shown on an expanded scale in Fig. 11. In this region the doppler response is good in terms of the sidelobe levels. At the doppler shift of -0.005, or more generally $1/(2\rho)$, the total phase shift across the uncompressed pulse is π and the peak response drops approximately 4 dB. At this doppler, there is a range-doppler coupling of 1/2 of a range cell with the result that the signal splits between two range cells. At a normalized doppler shift of -0.01, or in general $1/\rho$, there is a range-doppler coupling of one range cell resulting from a total phase shift of 2π radians across the uncompressed pulse, and the main peak response is nearly restored to full amplitude as shown in Fig. 9. This effect is cyclic and an approximate loss of nearly 4 dB is encountered when the total phase shift due to doppler is an odd multiple of 180°. This also occurs for the binary code except that the response is not cyclic and it monotonically decreases with frequency. Moreover, the troughs in the doppler response of the Frank code can be easily compensated by using an additional channel having a phase compensation of 180°. Also, it has been found that
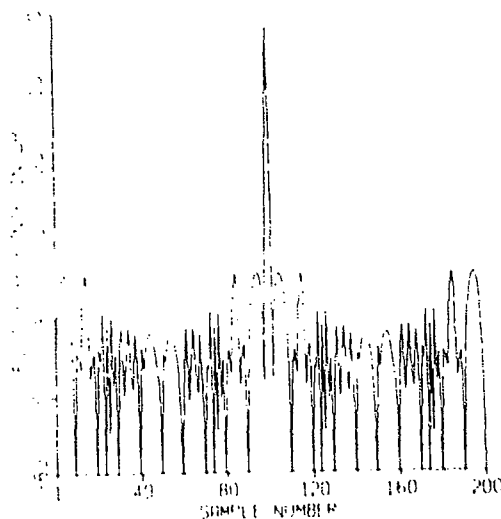

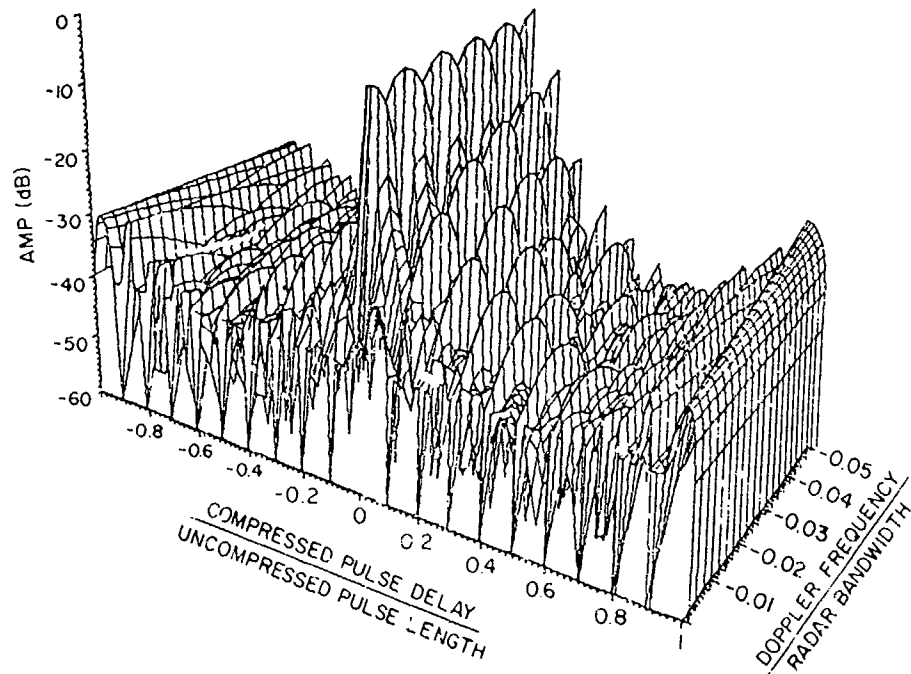Fig. 8 -- Compressed pulse of weighted Frank code

Fig. 9 — One hundred-element Frank code, partial ambiguity diagram
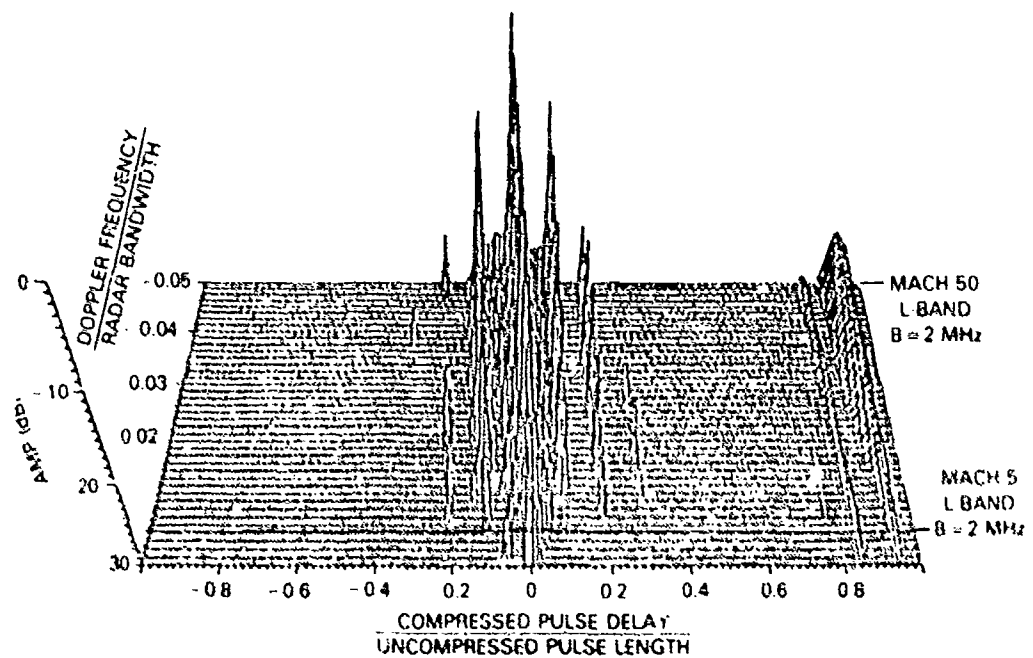

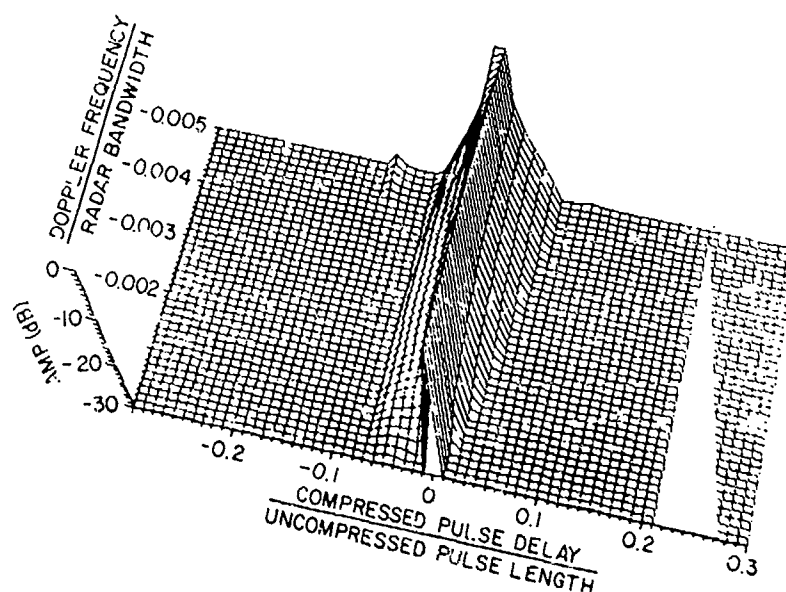Fig. 10 — One hundred-element Frank code, partial ambiguity diagram

Fig. 11 — Magnified ambiguity diagram of 100-element Frank code

that the use of weighting improves the sidelobes and reduces the variation in the mainlobe peak in the presence of doppler.

Figure 12 shows the output pulse for a 100-element-Frank-coded waveform having a doppler shift of -0.005 or a total phase shift of π across the uncompressed pulse. Figure 13 shows the effect of weighting on receive. In addition to the reduction of the end sidelobes, the mainlobe width has been reduced. These aspects of doppler compensation techniques are discussed in more detail in Ref. 10

Error Analysis

Computer simulations were performed to determine the sensitivity of the polyphase codes to phase and amplitude errors. The two types of errors considered were random errors in I and Q and quantization errors in I and Q which are encountered in A/D conversions.

Random Errors

Two types of random errors were considered as shown in Fig. 14. In each case independent, uniformly distribute errors in I and Q were generated over an interval $\pm x$. For the first type shown in Fig. 14(a), the error ϵ was determined by letting x be a given percentage of the nominal I or Q value for each code element phasor. The resultant vector is denoted as E_R. The other type of error ϵ', shown in Fig. 14(b) was generated as explained above, except that x was specified as a fixed error rather then a percentage of I or Q. In this case, the resultant vector is denoted by E_A. In determining E_R and E_A, the nominal signal amplitude is assumed to be unity.

Monte Carlo simulations were performed to determine the effect of the relative and absolute errors on the peak and average sidelobes of Frank codes with pulse compression ratios of 256 and 64. The results for $p = 256$ are shown in Fig. 15 with similar results obtaining for $p = 64$. Each point, other than for zero error, was obtained by taking an average of 100 compressed pulses to compute the indicated peak sidelobe and average sidelobe levels. The errors were assumed to occur on either transmission or reception but not both. The results of this simulation indicate that the
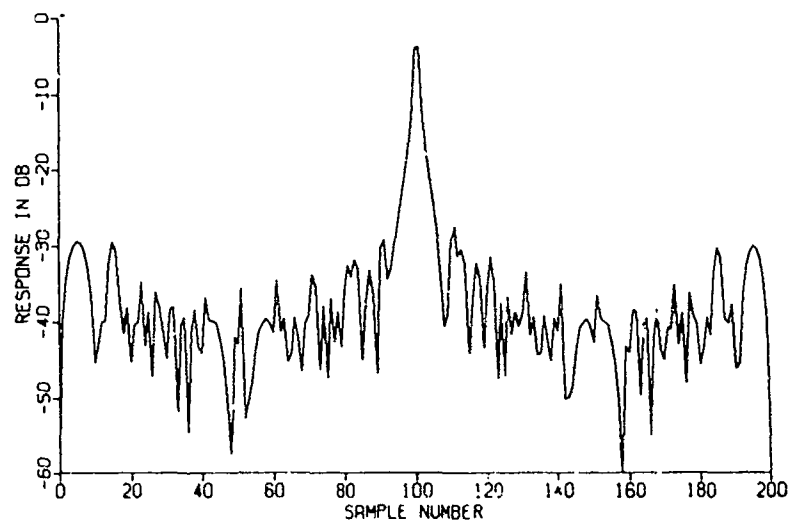
12

Fig. 12 — Compressed pulse of 100-element Frank code
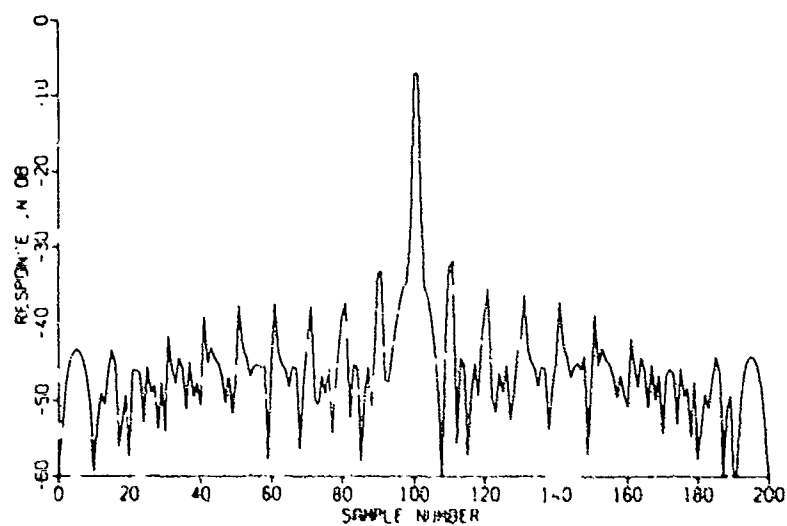doppler shifted by 0.005

Fig. 13 — Effects of weighting on compressed pulse of 100-element Frank code
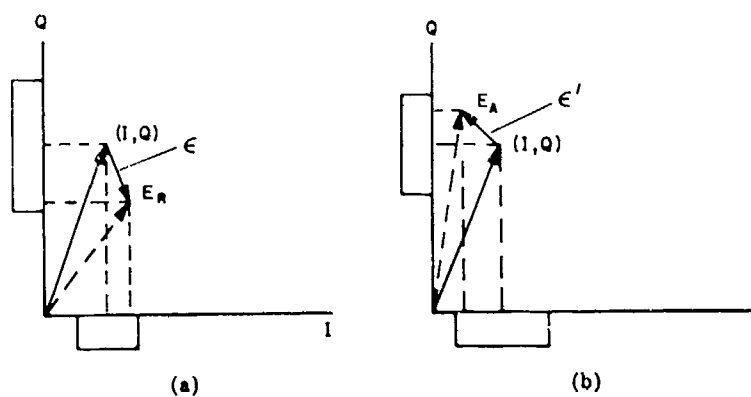doppler shifted by 0.005

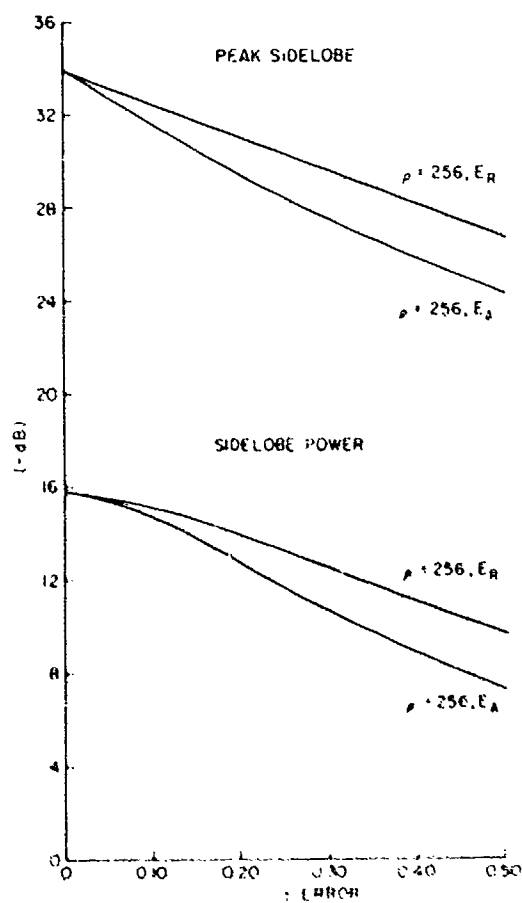(a)   (b)

Fig. 14 — Random errors

Fig. 15 — Frank polyphase-code error analysis

14

sidelobes are not sensitive to the errors. For example, for the absolute error case, an error distribution of ±0.10 results in approximately a 2-dB average degradation in the peak sidelobe and a 1.2-dB degradation in the average sidelobe power.

Quantization Errors

The results of the Monte Carlo simulations previously described indicate the robustness of the polyphase codes to random errors. To quantify the effects of quantization errors, computer simulations were performed. The average and peak sidelobes were determined for a symmetric A/D characteristic having the phase and amplitude specified within the accuracy of the quantization levels determined by the number of bits (including sign). Compression ratios of 144 and 36 were considered in the simulations, which did not include noise. It was assumed that the errors were due only to the A/D converters and that the matched-filter phases and amplitude were perfect. The results are shown in Fig. 16 where each curve exhibits a knee. The knee location is seen to vary the most between the $\rho = 36$ and $\rho = 144$ peak sidelobes. The general conclusion reached from these results is that the polyphase code is relatively insensitive to the number of bits beyond a certain number. Other considerations, such as dynamic range, may dictate the use of more bits than indicated in Fig. 16.

NEW POLYPHASE CODES [4,5]

Effects of Bandlimiting Prior to Pulse Compression

A Frank-coded waveform is depicted in Fig. 17(a) where the G_K's denote the phase groups corresponding to the sampled phases of a step-chirp waveform as previously discussed. Each group
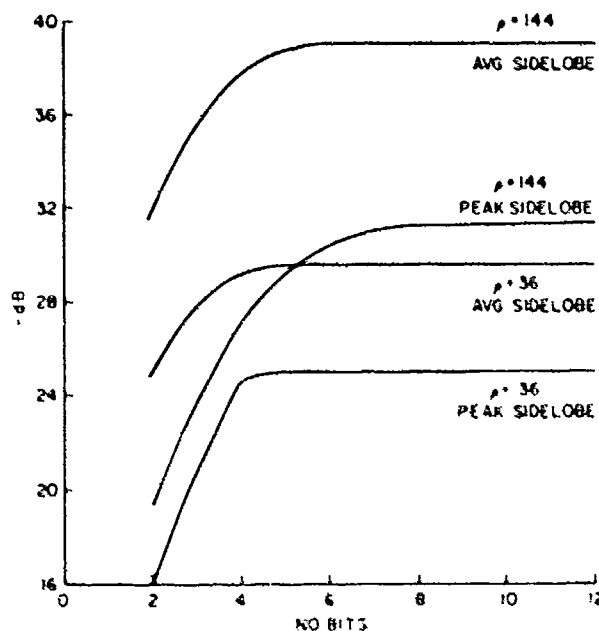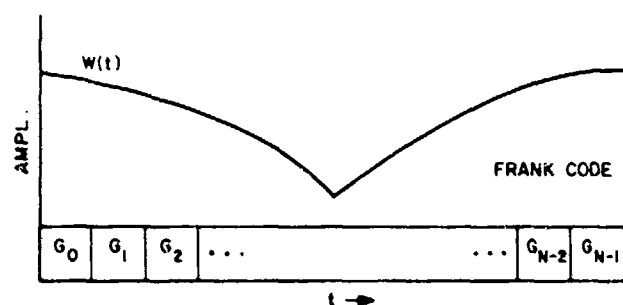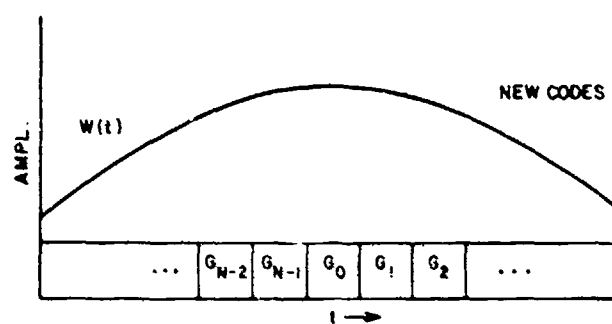

Fig. 16 — Frank-polyphase code, A/D quantization errors

Fig. 17 — Effect of bandlimiting before
pulse compression

consists of N vectors beginning with a vector at a phase angle of $0°$. The phase increments within the Kth group are

$$\Delta\phi_k = K\frac{360°}{N}. \tag{16}$$

Thus G_0 consists of N vectors at $0°$, G_1 has vectors separated by $360°/N$ until at the center of the coded waveform the phase increments approach or become $180°$ depending on whether N is odd or even. For phase increments greater than $180°$, the phases are ambiguous with the result that the phasors of phase group G_{N-K} are the conjugates of the phasors of phase group G_K so that the vectors have the same increments but rotate in opposite directions. The result is that the phase increments are small at the ends of the code and become progressively larger toward the center of the code where the increments approach $180°$ from opposite directions.

If a receiver is designed so that it has an approximate rectangular bandwidth corresponding to the 3-dB bandwidth of the received waveform, the received waveform becomes bandlimited and a mismatch occurs with the compressor. This bandlimiting would normally occur prior to sampling in the A/D conversion process in order to prevent noise foldover and aliasing. The result of any bandlimiting is to average (or smooth) the vectors constituting the coded waveform, and for the Frank code, a weighting $W(t)$ such as illustrated in Fig. 17(a) takes place due to the larger phase increments toward the middle of the code. This weighting causes an unfavorable mismatch with the compressor which results in a degradation of the sidelobes relative to the peak response.

16

New symmetrical codes have been found which have the common property that the phase groups with the small phase increments are at the center of the code and the larger increment groups progress symmetrically toward the ends of the code. This is illustrated in Fig. 17(b) where a favorable amplitude weighting resulting from pre-pulse compression bandlimiting is shown.

P1 and P2 Polyphase Cor:

The two new polyphase codes which tolerate bandlimiting are referred to as the P1 and P2 codes. The P1 code was derived from use of the previously described relationship between the Frank-code phases and those of a sampled step-chirp waveform. The desired symmetry, having the dc or small incremental phase group at the center of the code, can be achieved by determining the phases which result from placing the hypothetical synchronous oscillator at the center frequency of the step-chirp waveform. For an odd number of frequencies, the synchronous oscillator frequency corresponds to one of the waveform frequencies and the resultant phases are the same as the Frank code except the phase groups are rearranged as indicated in Fig. 17. If there is an even number of frequencies, the synchronous oscillator frequency placed at the center frequency does not correspond to one of the frequencies in the step-chirp signal. The phase of the ith element of the jth group is

$$\phi_{i,j} = -(\pi/N)[N - (2j - 1)][(j - 1)N + (i - 1)] , \tag{17}$$

where i and j are integers ranging from 1 to N.

An $N = 3$, P1, code is given by the sequence

$\phi_{1,1}$	$\phi_{2,1}$	$\phi_{3,1}$	$\phi_{1,2}$	$\phi_{2,2}$	$\phi_{3,2}$	$\phi_{1,3}$	$\phi_{2,3}$	$\phi_{3,3}$
0	$-2\pi/3$	$-4\pi/3$	0	0	0	0	$2\pi/3$	$4\pi/3$

which can be seen to be a rearranged Frank code with the zero frequency group in the middle.

The P2 code, which also has the desired features, is similar to the Butler matrix steering phases used in antennas to form orthogonal beams. The P2 code is valid for N even, and each group of the code is symmetric about 0 phase. The usual Butler matrix phase groups are not symmetric about 0 phase and result in higher sidelobes. For N even, the P1 code has the same phase increments, within each phase group, as the P2 code except that the starting phases are different. The ith element of the jth group of the P2 code is

$$\phi_{i,j} = \left[(\pi/2) \frac{N - 1}{N} - (\pi/N)(i - 1) \right] \left[N + 1 - 2j \right] , \tag{18}$$

where i and j are integers ranging from 1 to N as before. The requirement for N to be even in this code stems from the desire for low autocorrelation sidelobes. An odd value for N results in high autocorrelation sidelobes.

An $N = 4$, P2, code example is given by the sequence

$\phi_{1,1}$	$\phi_{2,1}$	$\phi_{3,1}$	$\phi_{4,1}$	$\phi_{1,2}$	$\phi_{2,2}$	$\phi_{3,2}$	$\phi_{4.2}$	$\phi_{1,3}$	$\phi_{2,3}$
$+9\pi/8$	$+3\pi/8$	$-3\pi/8$	$-9\pi/8$	$+3\pi/8$	$+\pi/8$	$-\pi/8$	$-3\pi/8$	$-3\pi/8$	$-\pi/8$

$\phi_{3,3}$	$\phi_{4,3}$	$\phi_{1,4}$	$\phi_{2,4}$	$\phi_{3,4}$	$\phi_{4,4}$
$+\pi/8$	$+3\pi/8$	$-9\pi/8$	$-3\pi/8$	$+3\pi/8$	$+9\pi/8$

This code has the frequency symmetry of the P1 code and also has the property of being a palindromic code which is defined as a code having symmetry about the center.

The ambiguity diagram of the P1 code for N odd is identical to that of the Frank code. For N even, the ambiguity diagrams of the P1 and P2 codes are similar to each other and to that of the Frank code.

Simulation of Precompression Bandwidth Limitations

The effect of a restricted bandwidth in the IF amplifiers and the I,Q detectors preceding analog-to-digital conversion and compression of the phase codes was simulated on a digital computer. The various codes to be compressed were over-sampled by 5 to 1 and sliding-window-averaged by 5, 7, and 10 to simulate the precompression bandwidth limitation. Only the results for the sliding-window average of 5 samples are presented here. Similar results were obtained for the other cases. The compressor phases were matched to tne input phases which existed prior to over-sampling. The resultant oversampled and averaged waveform was then sampled every fifth sample beginning with the first sample and sent to the compressor. To account for take time-of-arrival variations, the sliding-window average for the five-sample case was taken starting 4, 3, 2, 1, and 0 over-sample-periods ahead of the first received code element and sample correlation functions were developed for each case. Note that a match condition occurs for the latter case and otherwise a mismatch occurs.

The results of this study revealed that precompression bandwidth limitations were similar to amplitude weighting the frequency output ports of the digital filters in the compressor when the symmetrical P1 and P2 codes were employed and time-of-arrival variations were taken into consideration (Fig. 18). However, this was not the case when the Frank code was processed (Fig. 19). For the Frank coded waveform, the bandwidth limitation did not affect the dc group and had little effect on the highest frequency code group since it is the conjugate of the frequency code group closest to the dc term. As a consequence, precompression bandwidth limitation did not drop the far-out sidelobe caused by the dc group indexing into the highest frequency filter and vice versa.

Comparison of the sidelobes between the -30 and -40-dB lines of Figs. 18 and 19 shows that, for each corresponding time-of-arrival case, with the exception of the match condition shown in Part (c) of each figure, the sidelobes of the P2 code are lower than the Frank code, while the corresponding peak values are the same.

We mention at this point that although a sliding-window average was used to simulate the band limitation effects in this report, similar results would be expected for any other bandlimiting filter since the sidelobe reduction is due to the smoothing effect of the filter.
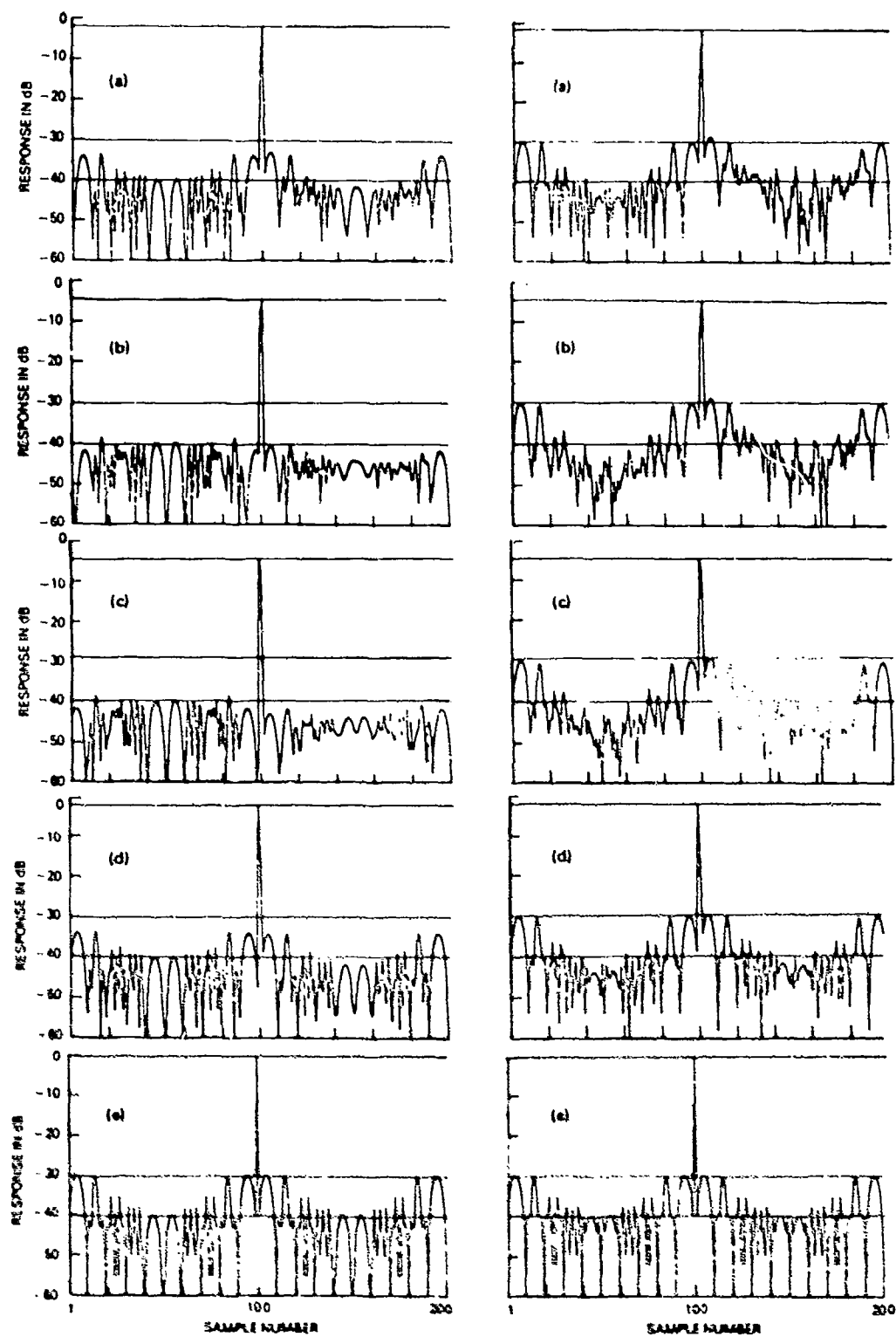
Fig 18 and 19 Effect of precompression band limitations on $N = 10$, P2 code and Frank code respectively, with 5 sample average started (a) 4, (b) 3, (c) 2, (d) 1, and (e) 0 samples ahead of first point to be sent to compressor

The average loss of the peak signal values shown in Figs. 18 and 19 is the same for both the Frank and P2 codes. Some of this loss can be attributed to the passband limitation while the remaining loss represents the loss due to time-of-arrival variation or range cusping. The passband limitation loss is due to the loss of the signal power contained in the sidelobes of the signal spectrum. The thermal-noise contribution is also reduced by the bandlimiting and is the same for each code in Figs. 18 and 19 which account for signal only. It is important to note, however, that the symmetrical P1 and P2 code sidelobes drop more than the peak due to precompression bandwidth limitation the sidelobes of the Frank code do not drop at all. This results in lower sidelobes in the new codes for the same signal-to-noise ratio loss due to the precompression bandwidth limitation.

APPLICATION OF POLYPHASE CODES

The polyphase codes discussed in this report may be used wherever pulse compression is needed and where the anticipated doppler-to-bandwidth ratio is less than approximately $1/(2p)$ corresponding to a range-doppler coupling of $1/2$ of a range cell. This doppler extent would apply to many search-radar and radar-mapping applications. These polyphase codes have much better doppler tolerance than the binary codes and have lower sidelobe levels.

The polyphase codes may be efficiently implemented to provide large pulse compression ratios, with normalized peak sidelobes given by $1/(p\pi^2)$. The achievable compression ratio is primarily limited by the signal bandwidth, which impacts on the A/D sampling rates and the digital circuit speeds. The polyphase pulse compressor does not become less efficient for long-duration waveforms as the analog acoustic delay-line compressors do.

For odd N, the P1 code, which is tolerant of precompression bandlimiting, can be implemented using FFT technology. This results in a considerable hardware savings for large p and allows the compression of different pulsewidths using the same processor.

The use of digital processing to compress the polyphase codes is compatible with digital MTI and pulse-doppler processing. As mentioned previously, the digital MTI can precede the digital pulse compressor to reduce the dynamic range requirements of the MTI without the need for multiple A/D and D/A conversions.

SUMMARY

The properties of Frank polyphase codes have been investigated in detail and extended. It was shown how the Frank code can be conceptually derived by appropriately sampling a step-chirp waveform and how the Frank and new polyphase codes are useful for doppler-to-bandwidth ratios less than approximately $1/(2p)$. Doppler compensation techniques were presented to improve the performance of the polyphase codes. Also it was found that the polyphase codes are not very sensitive to amplitude and phase errors.

New polyphase codes were described which have more tolerance to precompression bandlimiting than the Frank codes. The precompression bandlimiting acts as a weighting on the Frank codes, which increases the sidelobe levels relative to the peak. The normalized sidelobe levels of the new codes are reduced by the effective weighting caused by precompression bandlimiting.

REFERENCES

1. F. E. Nathanson, "Radar Design Principles." New York: McGraw-Hill, 1969.

2. M. I. Skolnik, "Introduction to Radar Systems," New York: McGraw-Hill, 1980.

3. R. S. Berkowitz, "Modern Radar Analysis, Evaluation, and System Design," New York: Wiley and Sons, Inc., 1965 p. 98.

4. B. L. Lewis and F. F. Kretschmer, Jr., "A New Class of Pulse Compression Codes and Techniques," NRL Report #8387, March 26, 1980.

5. B. L. Lewis and F. F. Kretschmer, Jr., "A New Class of Polyphase Pulse Compression Codes and Techniques," IEEE Transactions on Aerospace and Electronic System," May 1981, AES-17, pp. 364-372.

6. C. Cook and M. Bernfield, "Radar Signals, An Introduction to Theory and Applications," New York: Academic Press, 1967.

7. R. L. Frank, "Polyphase Codes With Good Nonperiodic Correlation Properties," IEEE Transactions on Information Theory, June 1963, IT-9, pp. 43-45.

8. M. H. Ackroyd and F. Ghani, "Optimum Mismatched Filters for Sidelobe Suppression," IEEE Transactions on Aerospace and Electronic Systems, March 1973, AES-9, No. 2, pp. 214-218.

9. U. Somaini and M. H. Ackroyd, "Uniform Complex Codes With Low Autocorrelation Sidelobes," IEEE Transactions on Information Theory, Sept. 1974, IT-20, pp. 689-691.

10. F. F. Kretschmer, Jr. and B. L. Lewis, "Doppler Induced Losses in a Frank Code Pulse Compression System and Correction Techniques," Submitted to IEEE Transactions on Aerospace and Electronic Systems.